BIOCHEMICAL AND BIOPHYSICAL RESEARCH COMMUNICATIONS **224,** 191–198 (1996)
ARTICLE NO. 1006

Chemically Synthesised Human Immunodeficiency Virus P7 Nucleocapsid Protein Can Self-Assemble into Particles and Binds to a Specific Site on the tRNA^{Lys,3} Primer

Hasan Al-Ghusein,* Haydn Ball,† Gabor L. Igloi,‡ Armstrong Gbewonyo,* Anthony R. M. Coates,* Paolo Mascagni,† and Michael M. Roberts*,[1]

**Division of Molecular Microbiology, St. George's Hospital Medical School, Cranmer Terrace, London SW17 ORE, United Kingdom; †Department of Chemistry, Italfarmaco Research Centre, Via Lavoratori, 54, Cinisello Balsamo 20092, Milan, Italy; and ‡Institut für Biologie III, Universität Freiburg, Schänzle-Strasse 1, D-7800 Freiburg, Germany*

Received May 29, 1996

The zinc-bound form of the human immunodeficiency virus type 1 (HIV-1) nucleocapsid protein, p7, aggregates into particles visible by electron microscopy. The HIV primer tRNA^{Lys,3} forms similar high molecular weight complexes with p7 that are also detected by gel mobility shift assays. RNA oligonucleotides of the three stem-loop structures in tRNA^{Lys,3} were assayed for the competitive inhibition of p7-tRNA^{Lys,3} binding by the intensities of free tRNA^{Lys,3} bands on native gels. This reveals that the p7 binds specifically to the central domain of tRNA^{Lys,3} where the D and TψC loops come together, but not the anticodon stem-loop. © 1996 Academic Press, Inc.

Both Gag and Gag-Pol polyproteins of HIV are processed by the viral proteinase into the individual protein components (1), which includes the nucleocapsid protein, p7. The p7 was also shown to bind to the tRNA^{Lys,3} primer and anneal it to the 18-base complementary sequence on the primer binding site of the genomic RNA (2). The p7 performs this by its tRNA unwinding (3) and renaturation activity (4). Specific binding of p7 to tRNA^{Lys,3} was demonstrated by competition with other tRNAs (5). Subsequently, the anticodon loop of tRNA^{Lys,3}, which had previously been proposed as a specific binding site for p7 (6) on the basis of crosslinking and RNase digestion studies did not show any specific binding using fluorescence techniques (7).

In this investigation we examine the assembly of zinc-bound synthetic HIV p7 alone and with tRNA^{Lys,3} primer by observing particle formation by electron microscopy. We show how the formation of p7-tRNA^{Lys,3} macromolecular aggregates is utilized in a gel mobility shift assay (8) to study the competitive inhibition of p7-tRNA^{Lys,3} binding described here. We have located a specific HIV p7 binding site on tRNA^{Lys,3} by studying the effect of RNA oligonucleotides representing the stem-loop structures of tRNA^{Lys,3} on p7-tRNA^{Lys,3} binding.

MATERIALS AND METHODS

Preparation of tRNA^{Lys,3}. Two complementary DNA oligonucleotides were chemically synthesised (Fig. 1A) comprising the gene corresponding to the tRNA^{Lys,3} together with the promoter sequence specific for the phage T7 RNA polymerase and appropriate restriction sites to permit cloning into a bacterial plasmid. Following enzymatic 5′ phosphorylation, the oligonucleotides were ligated to DNA from puc19 into the KpnI/HindIII site and transformation of *Escherichia coli* TG1 cells was performed. Positive clones, identified by restriction mapping, were confirmed by

[1] To whom correspondence should be addressed. Fax: 44-181-682-1320.

Abbreviations: DDP, diamminedichloroplatinum; HIV-1, human immunodeficiency virus type 1; PBS, primer binding site; RT, reverse transcriptase; SDS-PAGE, sodium dodecyl sulphate polyacrylamide gel electrophoresis; TBE, 0.089M Tris/borate, 2mM EDTA, pH 8.3; t-BOC, tertiary butyloxycarbonyl; TFA, trifluoroacetic acid.

0006-291X/96 $18.00
Copyright © 1996 by Academic Press, Inc.
All rights of reproduction in any form reserved.

A

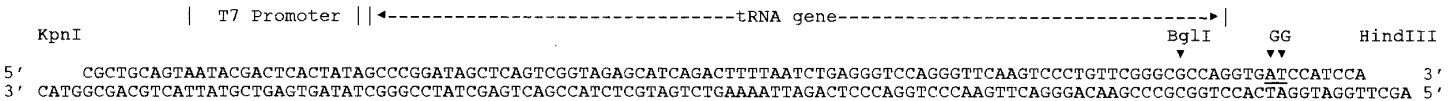
T7 Promoter
tRNA gene
KpnI
BglI
GG
HindIII
5′ CGCTGCAGTAATACGACTCACTATAGCCCGGATAGCTCAGTCGGTAGAGCATCAGACTTTTAATCTGAGGGTCCAGGGTTCAAGTCCCTGTTCGGGCGCCAGGTGATCCATCCA 3′
3′ CATGGCGACGTCATTATGCTGAGTGATATCGGGCCTATCGAGTCAGCCATCTCGTAGTCTGAAAATTAGACTCCCAGGTCCCAAGTTCAGGGACAAGCCCGCGGTCCACTAGGTAGGTTCGA 5′

B

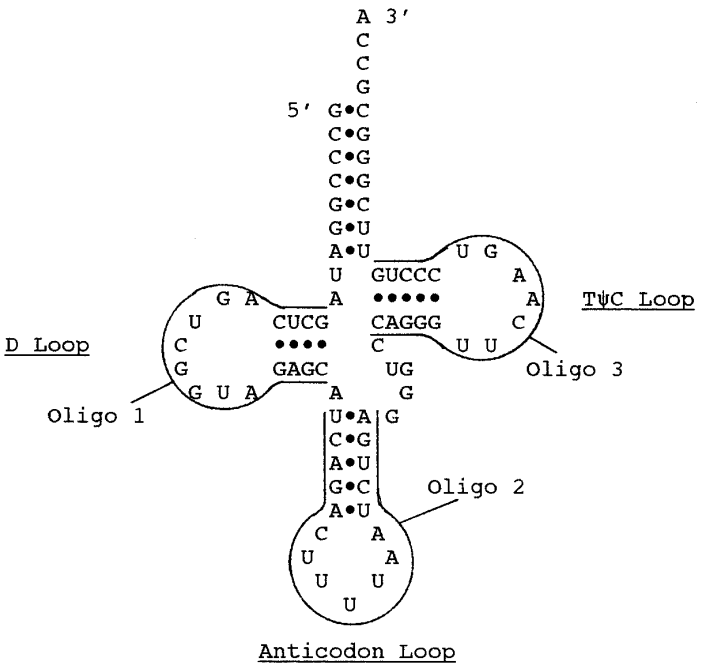
A 3′
5′ G•C
TψC Loop
D Loop
Oligo 1
Oligo 3
Oligo 2
Anticodon Loop

sequence analysis and the appropriate plasmid was isolated. To obtain an *in vitro* transcript identical to the sequence of the native $tRNA^{Lys,3}$, restriction cleavage at exactly the 3′ terminus was necessary. A BglI site (recognition sequence 5′ GCCNNNN|NGGC) was introduced by mutagenesis in the region 3′ to the terminus. Cleavage with this enzyme then gave rise to the sequence 3′ . . .GGT 5′ on the lower (coding) strand, with the corresponding correct CCA terminus in the transcript. Transcription was performed on the EcoRI/BglI restricted plasmid in the presence of high concentrations of nucleoside triphosphates and commercial T7 RNA polymerase (9). Furthermore, inclusion of GMP in the incubation ensured that the 5′ end bore a single phosphate.

Purification of $tRNA^{Lys,3}$. The $tRNA^{Lys,3}$ was denatured in gel loading buffer (95% v/v formamide, 20 mM EDTA, 0.05% w/v bromophenol blue, 0.05% w/v xylene cyanol FF) at 85°C for 5 min then electrophoresed at 100 V on a pre-run 10% polyacrylamide gel (PAG) in 8.3 M urea and TBE (0.089 M Tris/borate, 2 mM EDTA, pH 8.3) from the SequaGel kit (National Diagnostics) for inhibition assays, or 0.04 M Tris/acetate buffer, pH 8.0 for gel mobility shift assays. Gels were stained 10 min in ethidium bromide solution and visualised under UV light. The Bio101 Rnaid kit was used to extract the $tRNA^{Lys,3}$ from the gel according to the manufacturer's instructions. Absorbance measurements were taken at 260 nm to estimate the $tRNA^{Lys,3}$ concentration using an extinction coefficient of 6.25×10^5 M^{-1} cm^{-1} (7).

Radiolabeling of $tRNA^{Lys,3}$. After dephosphorylation, the $tRNA^{Lys,3}$ was heated at 95°C for 5 min then cooled on ice. The $tRNA^{Lys,3}$ was 5′ labeled with [γ-^{32}P]ATP using Ready-To-Go T4 polynucleotide kinase (Pharmacia) according to the manufacturer's instructions. 2.5 volumes of ethanol and 0.02 volumes of glycogen (Appligene) were added to precipitate the $tRNA^{Lys,3}$ at −20°C overnight. The precipitate was centrifuged at 14,000 rpm for 30 min at 4°C in an Eppendorf microcentrifuge. The pellet was washed 2× with 70% v/v ethanol, vacuum dried, resuspended in gel loading buffer in RNase-free water, then purified by PAG as described above.

Oligonucleotides. Three specific RNA oligonucleotides (oligos 1-3) representing the three stem-loop structures of $tRNA^{Lys,3}$ in Fig. 1B were synthesised and purified by Oswel, and one non-specific deoxyoligonucleotide control (5′-TCGTCACAATAAAGAGAATTCGCTAATCAC-3′) was synthesised and purified by Genosys. Oligo 1 (5′-GCUCAGUCGGUAGAGC-3′, bases 10-25) includes the D loop, oligo 2 (5′-UCAGACUUUUAAUCUGA-3′, bases 27-43) includes the anticodon loop, and oligo 3 (5′-CAGGGUUCAAGUCCCUG-3′, bases 49-65) includes the TψC loop.

Preparation, purification and analysis of HIV p7. The 71 amino acid HIV p7 sequence from the LAI isolate (10) was chemically synthesised on solid phase using t-BOC chemistry. To avoid oxidation of the cysteine residues in p7, all procedures were performed under argon. The p7 was purified batchwise by reversed-phase HPLC with two successive acetonitrile-water gradients in 0.1% TFA on a semi-preparative 220×10 mm 10 μm C4 Vydac column with a 3 ml/min flow rate as described (2). The elution profile of purified p7 was checked at 220 nm on an analytical C18 Vydac column with an acetonitrile-water gradient in 0.1% TFA from 0% to 30% acetonitrile in 60 min at 1 ml/min. The purified p7 eluted as a single peak at 27% acetonitrile. The amino acid composition of p7 is in good agreement with the expected values. SDS-PAGE of p7 on a Pharmacia High Density PhastGel (20% polyacrylamide, 30% ethylene glycol) shows a single band at the expected position of about 10kDa. Mass spectrometry of p7 using the electrospray technique (ETH, Zürich) gives a molecular weight of 8286.0 (calculated, 8286.7). N-terminal sequencing (ETH, Zürich) correctly identified each amino acid up to Trp 37. The p7 was prepared as a 0.22 mM stock solution in 1 mM $ZnSO_4$, pH 5.0, purged with argon and used in all experiments. The absorbance of this stock solution, diluted 1:10 with 25 mM Tris/HCl, 60 mM NaCl, pH 7.5 (binding buffer) was 0.28 at 280 nm. This is in agreement with the expected extinction coefficient for p7, ϵ=12,700 $M^{-1}cm^{-1}$ (7). The same absorbance measurements were used to determine the concentrations of p7 solutions after dialysis. The zinc content of the stock solution after dialysis against Tris/HCl/NaCl buffer, pH 7.5 as described (11) was determined by atomic absorption spectroscopy and a p7:Zn molar ratio of 1:2 was confirmed, as expected for p7, which has two zinc-binding sites (11). The p7 used in these experiments is therefore of adequate purity and is in the zinc-bound form.

Gel mobility shift assay. The p7 stock solution was dialysed against 25 mM Tris/HCl, 60 mM NaCl, 5 mM $MgCl_2$, pH 7.5 to give a 0.147 mM solution of p7. The p7 was diluted to a range of concentrations (0.07-4.41 μM) that were incubated with 0.1 μM [γ-^{32}P]ATP labeled $tRNA^{Lys,3}$ in 10 μl of the same buffer for 10 min at room temperature. The reaction products were electrophoresed at 100 V for 3 h on a 5% PAG (60:1 acrylamide to bis-acrylamide) with 0.1% NP-40 in 0.5×TBE, and analysed by autoradiography of the dried gel.

FIG. 1. $tRNA^{Lys,3}$ and its synthetic fragments used to study p7-$tRNA^{Lys,3}$ binding. (A) The two complementary oligonucleotides cloned into *E. coli* TG1 cells for the *in vitro* expression of $tRNA^{Lys,3}$, as described in Materials and Methods. The KpnI and HindIII restriction sites for ligation into puc19 are indicated at each end. The nucleotides AT (underlined) were mutated to GG to engineer the BglI site (indicated by ▼) for transcription of the $tRNA^{Lys,3}$. (B) The secondary structure of the *in vitro* expressed $tRNA^{Lys,3}$ containing the unmodified bases. The locations of the chemically synthesised RNA oligonucleotides (oligos 1−3) with respect to the stem-loop structures of $tRNA^{Lys,3}$ are indicated by solid lines enclosing the stem-loops.

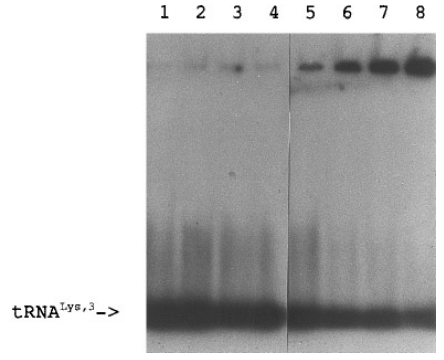

FIG. 2. The precipitation of tRNA^{Lys,3} by p7 into high molecular weight complexes. Autoradiograph of gel mobility shift assay on 0.1 μM ^{32}P-labeled tRNA^{Lys,3} incubated with p7 concentrations of 0.07 μM (lane 1), 0.15 μM (lane 2), 0.29 μM (lane 3), 0.44 μM (lane 4), 0.735 μM (lane 5), 1.47 μM (lane 6), 2.94 μM (lane 7), and 4.41 μM p7 (lane 8) followed by electrophoresis on native 5% PAG as described in Materials and Methods.

Inhibition of p7-tRNA^{Lys,3} binding. HIV p7 (0.22 mM) in $ZnSO_4$ (1 mM), pH 5.0 was diluted 1:20 in 0.5× binding buffer, 4 u RNasin (Promega), and 1 μg of denatured salmon sperm DNA (Sigma), then incubated 10 min at room temperature. 21 pmoles of the specific oligonucleotides (oligos 1-3) or 10 pmoles of the non-specific deoxyoligonucleotide (DNA oligo) was added. This was followed by a further 10 min incubation at room temperature. The [γ-^{32}P]ATP labelled tRNA^{Lys,3} (0.14 pmoles) was added and the whole cocktail incubated for 30 min at 37°C in a final volume of 20 μl. The effective mononucleotide concentration of all the oligos is approximately 15μM. The incubated samples were mixed with 2 μl glycerol and loaded onto a native 8% PAG (80:1 acrylamide to bis-acrylamide) and electrophoresed in 0.5×TBE for 3 h after a pre-run for 90 min at 100 V. The gel was dried and autoradiographed.

Electron microscopy. Samples were prepared from HIV p7 (0.22 mM) in $ZnSO_4$ (1 mM), pH 5.0 diluted 1:1000 in water and stored 4 days at 4°C. p7 diluted to 1:100 with tRNA^{Lys,3} (0.6 μM) in binding buffer was incubated 10 min or more at room temperature. Samples were positively stained with 2% uranyl formate, pH 8.9. Specimens were examined on Formvar carbon-coated grids with a JEOL JEM 1200EX Mk II electron microscope operated at 100 kV accelerating voltage with a primary magnification of 50000.

RESULTS

Aggregation of p7 with tRNA^{Lys,3}. In native polyacrylamide gels, complex formation between HIV p7 and tRNA^{Lys,3} is observed to occur as a shift in the tRNA^{Lys,3} band to a precipitate in the loading well. The precipitation with 0.1 μM tRNA^{Lys,3} increases in the p7 concentration range of 0.735-4.41 μM with or without 5 mM $MgCl_2$ (Fig. 2). This is confirmed by high molecular weight aggregates observed in positive stained uranyl formate electron micrographs of mixed tRNA^{Lys,3}-p7 preparations in binding buffer. Solutions of 0.6 μM tRNA^{Lys,3} with increasing concentrations of p7 show increasing states of aggregation. With 2.2 μM p7, particles up to 40 nm in diameter are formed, which self-assemble into chain-like structures (Fig. 3A). Electron micrographs of the p7 stock solution diluted in water to 0.22 μM show three types of particle that form out of solution after a few days: (a) rod-shaped particles 8 nm in diameter and up to 250 nm in length and (b) 20 nm in diameter and 20 nm-100 nm in length and (c) oval particles up to 40 nm across (Fig. 3B). All particles have a hollow cylindrical core about 4 nm in diameter. Only the oval particles in Fig. 3B resemble the p7-tRNA^{Lys,3} particles in Fig. 3A except in the latter the central cavity appears to be filled and they are less aggregated. Interestingly, the same 0.22 μM p7 solution prepared in binding buffer or 10 mM EDTA showed more disrupted material and some oval structures (data not shown). The addition of 0.6 μM tRNA^{Lys,3} to these p7 preparations dramatically increases the number of particles. Electron micrographs of tRNA^{Lys,3} alone showed nothing, indicating that the aggregation was purely due to p7 association and tRNA^{Lys,3} complexation.

Specific inhibition of p7-tRNA^{Lys,3} binding by RNA oligonucleotides. The inclusion of dena-

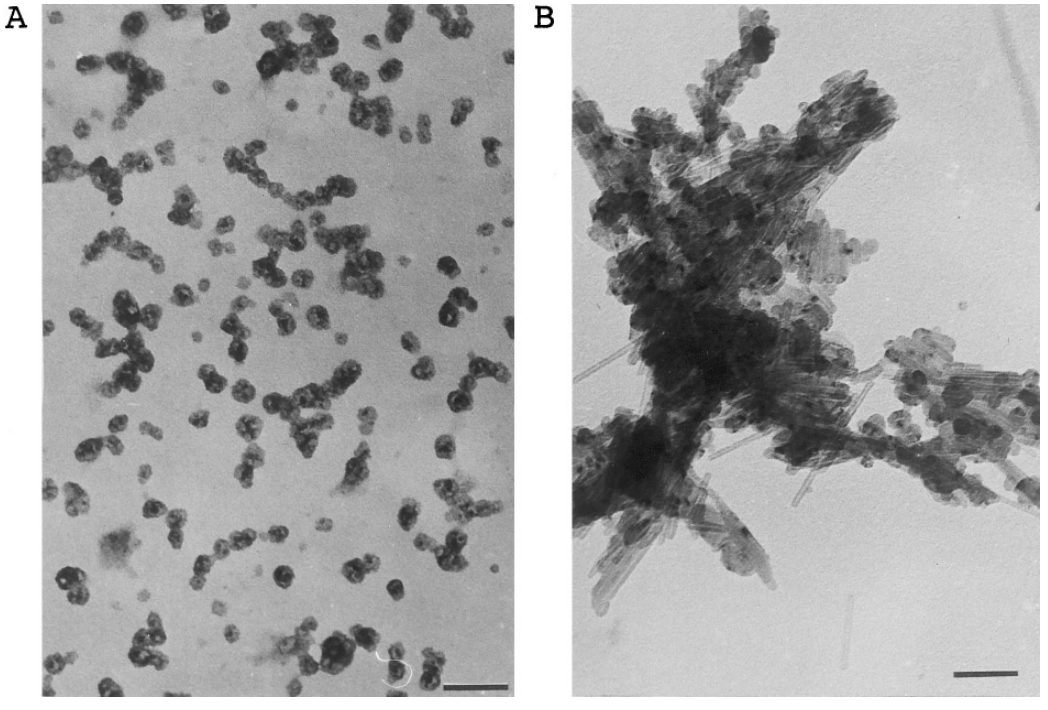

FIG. 3. Assembly of p7 and p7/tRNA^{Lys,3} complexes into particles. Positive-stained electron micrographs of (A) 0.6 μM tRNA^{Lys,3} with 2.2 μM p7 in binding buffer and (B) 0.22 μM zinc-bound HIV p7 in water. Bars represent 100 nm; original magnification was $\times$50,000.

tured salmon sperm DNA into the p7-tRNA^{Lys,3} binding cocktail to block the non-specific interactions between p7 and tRNA^{Lys,3} made it possible to observe the effects of oligos 1-3 on specific interactions between p7 and tRNA^{Lys,3}. Under these conditions, the disappearance of the radiolabelled tRNA^{Lys,3} bands migrating into the native gel due to complexation with p7 is inhibited by the preincubation of 11 μM p7 with oligos 1-3 and salmon sperm DNA prior to the addition of 0.01 μM tRNA^{Lys,3}. The degree of inhibition by the oligos 1-3 increases with the restoration of the intensity of the free migrating tRNA bands. This is illustrated in Fig. 4, where incubation with oligo 1 gives the greatest tRNA^{Lys,3} band intensity (lane 4),

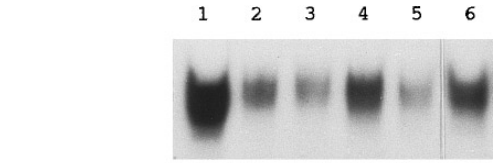

Oligo 1	–	–	–	+	–	–
Oligo 2	–	–	–	–	+	–
Oligo 3	–	–	–	–	–	+
DNA oligo	–	–	+	–	–	–
HIV p7	–	+	+	+	+	+

FIG. 4. Competitive inhibition of p7/tRNA^{Lys,3} binding by tRNA^{Lys,3}-specific oligonucleotides. Autoradiograph of uncomplexed ^{32}P-labeled tRNA^{Lys,3} from incubations of 0.01 μM tRNA^{Lys,3} with 11 μM HIV p7 in the presence of different oligonucleotides at effective mononucleotide concentrations of 15 μM following electrophoresis on native 8% PAG as described in Materials and Methods.

followed by oligo 3 (lane 6). Incubation with oligo 2 gives a $tRNA^{Lys,3}$ band intensity (lane 5) comparable to that obtained with the DNA oligo (lane 3). This indicates that oligos 1 and 3 inhibit p7-$tRNA^{Lys,3}$ binding, and oligo 2 and the DNA oligo have no effect on p7-$tRNA^{Lys,3}$ binding. The incubations were performed in parallel with the DNA oligo to exclude the possibility of a random sequence interfering with p7-$tRNA^{Lys,3}$ binding.

DISCUSSION

The conditions under which nonspecific binding of p7 to $tRNA^{Lys,3}$ was reported included the use of p7 at concentrations too low for aggregation to occur (7). While we accept the findings of those investigators, we claim that at higher p7 concentrations and using an alternative approach by analysing the binding of p7 to selected parts of $tRNA^{Lys,3}$ there are definite observable differences. In the HIV virion, the concentration of p7 is about 5 mM (7), and this is clearly interacting with the $tRNA^{Lys,3}$ in an aggregated form. Under these conditions, specific interactions between p7 and $tRNA^{Lys,3}$ may be important. The gel mobility assay in Fig. 2 shows that $tRNA^{Lys,3}$ is precipitated in increasing amounts as the p7 concentration is increased from 0.735 μM to 4.41 μM due to the formation of p7-$tRNA^{Lys,3}$ aggregates that are visible in electron micrographs (Fig. 3A). The use of excess salmon sperm DNA in Fig. 4 immobilises the nonspecifically bound p7 and therefore provides a better contrast in competition assays between specific and nonspecific binding sites on $tRNA^{Lys,3}$ by p7.

Oligos 1 and 3 containing the D and TΨC loops inhibit p7-$tRNA^{Lys,3}$ binding whereas oligo 2 containing the anticodon loop is unable to inhibit p7-$tRNA^{Lys,3}$ binding (Fig. 4). The base-pairing between the D and TψC loops forms an important part of the tertiary structure of all tRNAs (12), and are joined at the central domain of the tRNA structure. The differences in inhibition indicate that p7 binds specifically to the folded $tRNA^{Lys,3}$ structure at this central domain. The dissociation of the D-TψC loop base pairing is reported to be the first stage in the melting of the tertiary structure of tRNA (13). The nucleic acid renaturation activity of HIV p7 (4) together with the affinity of p7 for the D and TψC loops could result in the separation of both loops as a first step in the unfolding of $tRNA^{Lys,3}$ (3), followed by unwinding of the TψC stem-loop and isoacceptor stem for the annealing of $tRNA^{Lys,3}$ to the PBS on the genomic HIV RNA (2). Interestingly, the reverse transcriptase (RT) was shown to bind to the same central domain of $tRNA^{Lys,3}$ based on gel retardation studies on $tRNA^{Lys,3}$ mutants (14). The requirement of RT for $tRNA^{Lys,3}$ annealing to viral RNA was also demonstrated (14). These findings suggest that annealing of the $tRNA^{Lys,3}$ primer to the PBS is associated with binding of RT or p7 to this central domain of $tRNA^{Lys,3}$. The binding of RT and p7 to $tRNA^{Lys,3}$ could be cooperative, since a p15-$tRNA^{Lys,3}$-RT complex has been formed *in vitro* and the binding of p15 to $tRNA^{Lys,3}$ appears to be stabilised when RT is present (2).

In light of our observations, we find the report of the p7 chemically cross-linked to the the anticodon loop puzzling (6). Similarly, the binding of RT to $tRNA^{Lys,3}$ at the D and TψC loops (14) could not confirm the results of the chemical cross-linking studies, where the RT was found to be cross-linked to the anticodon loop only (5,15). The cross-linking agent used was *trans*-diamminedichloroplatinum (*trans*-DDP). In the crystal structure of $tRNA^{Phe}$ derivatised with *trans*-DDP (16,17), one *trans*-DDP molecule binds on the anticodon loop which is an exposed location favourable for cross-linking to protein. *trans*-DDP may also attach to an exposed location on the anticodon loop of $tRNA^{Lys,3}$. This would explain why both HIV p7 and RT cross-link to the anticodon loop in preference to other locations (5,6,15). Furthermore, in HIV p7, crosslinking is only possible via the Cys and His amino acids in the conserved zinc-binding domains (18,19). The Cys and His amino acids on p7 coordinate zinc in a pocket within a coiled polypeptide conformation in the native zinc-bound p7 structure (20), and are thus inaccessible to cross-linking. It is not the Cys or His amino acids that are important for the direct recognition and binding of specific RNA sequences, but the aromatic amino acids

on the surface of the zinc-binding domains in the zinc-bound form (21). Furthermore, it is the basic amino acids on p7 that are important for the annealing of $tRNA^{Lys,3}$ to viral RNA (22). Consequently, the biologically important p7-$tRNA^{Lys,3}$ interactions are not necessarily compatible with the mechanism of protein-RNA cross-linking by *trans*-DDP.

The tendency of zinc-bound HIV p7 to aggregate into high molecular weight complexes may account for the precipitation of $tRNA^{Lys,3}$ which occurs in the presence of HIV p7. However, the increase in particles with $tRNA^{Lys,3}$ suggests that there is a lot of soluble p7 that is precipitated by $tRNA^{Lys,3}$. The aggregation of p7-$tRNA^{Lys,3}$ complexes has been reported previously as a turbidity that appears in solution above a p7 concentration of 1.5 μM (7). This is in agreement with the gel mobility shift assay in Fig. 2, where p7-$tRNA^{Lys,3}$ aggregates start to precipitate in the range of 0.735-4.41 μM p7, and with the aggregation of p7-$tRNA^{Lys,3}$ particles into chain-like structures at 2.2 μM p7 in Fig. 3A. The similar size and shape of these p7-$tRNA^{Lys,3}$ particles to the oval particles in Fig. 3B suggests that only this type of p7 assembly is favourable for $tRNA^{Lys,3}$ complexation.

Rod-shaped particles 50 nm in diameter formed from the *in vitro* assembly of the HIV (p24-p7) fusion protein only with RNA (2700-7000 bases) (23). The HIV (p24-p7) was prepared in EDTA and so would not contain zinc. The ability of our HIV p7 to self-assemble into rod-shaped particles without RNA could be due to the absence of p24 capsid protein or the bound zinc, since a 0.22 μM p7 solution treated with 10 mM EDTA showed very few of the rod-shaped particles in Fig. 3B (data not shown). The 4 nm cylindrical cavity in these rod-shaped particles may be formed to accommodate the viral RNA, but this has to be established by further studies of p7-RNA complexes.

In conclusion, we have shown that chemically synthesised HIV p7, in the zinc-bound form without RNA can self-assemble into morphologically distinct particles visible by electron microscopy. Above a critical p7 concentration, aggregation, particle formation and $tRNA^{Lys,3}$ complexation occurs. Zinc-bound HIV p7 at aggregation concentrations binds specifically to the central domain containing the D and TψC loop sequences of the folded $tRNA^{Lys,3}$ primer, but not to the anticodon stem-loop in the presence of nonspecific competitor DNA. These specific interactions may be important for the unwinding and annealing of the $tRNA^{Lys,3}$ primer to the viral RNA. The position of the p7 binding sites on $tRNA^{Lys,3}$ remains to be explored more precisely by monitoring the effects of mutations in the D and TψC stem-loops on p7-$tRNA^{Lys,3}$ binding in gel mobility assays, as for RT (14). The role of p7-$tRNA^{Lys,3}$ binding in annealing to viral RNA, reverse transcription, $tRNA^{Lys,3}$ incorporation and viral replication could be investigated with similar mutants. The specific binding site for p7 on the central domain of $tRNA^{Lys,3}$ could also be defined more precisely by selecting a narrower choice of competing oligos. The identification of specific RNA oligonucleotides here that inhibit p7-$tRNA^{Lys,3}$ complexation could lead to the development of further compounds that selectively prevent HIV primer annealing and may have therapeutic value.

ACKNOWLEDGMENTS

We thank Dr. Milan V. Nermut and Dr. Sean Heaphy for helpful discussion on the p7 aggregation and p7-$tRNA^{Lys,3}$ binding. The assistance of the laboratory staff at Italfarmaco is gratefully acknowledged. We are also grateful to Miss E. Hutchinson for the zinc analyses on HIV p7. This work was supported by Grant G9304370 from the Medical Research Council.

REFERENCES

1. Henderson, L. E., Bowers, M. A., Sowder, R. C., II, Serabyn, G. W., Johnson, D. G., Bess, J. W., Jr., Arthur, L. O., Bryant, D. K., and Fenselau, C. (1992) *J. Virol.* **66,** 1856–1865.
2. de Rocquigny, H., Ficheux, D., Gabus, C., Fournié-Zaluski, M.-C., Darlix, J.-L., and Roques, B. P. (1991) *Biochem. Biophys. Res. Commun.* **180,** 1010–1018.
3. Khan, R., and Giedroc, D. P. (1992) *J. Biol. Chem.* **267,** 6689–6695.

4. Dib-Hajj, F., Khan, R., and Giedroc, D. P. (1993) *Protein Sci.* **2,** 231–243.
5. Barat, C., Lullien, V., Schatz, O., Keith, G., Nugeyre, M. T., Grüninger-Leitch, F., Barré-Sinoussi, F., LeGrice, S. F. J., and Darlix, J.-L. (1989) *EMBO J.* **8,** 3279–3285.
6. Barat, C., Schatz, O., LeGrice, S., & Darlix, J.-L. (1993) *J. Mol. Biol.* **231,** 185–190.
7. Mély, Y., de Rocquigny, H., Sorinas-Jimeno, M., Keith, G., Roques, B. P., Marquet, R., and Gérard, D. (1995) *J. Biol. Chem.* **270,** 1650–1656.
8. Fried, M., and Crothers, D. M. (1981) *Nucleic Acids Res.* **9,** 6505–6525.
9. Milligan, J. F., Groebe, D. R., Witherell, G. W., and Uhlenbeck, O. C. (1987) *Nucleic Acids Res.* **15,** 8783–8798.
10. Wain-Hobson, S., Sonigo, P., Danos, O., Cole, S., and Alizon, M. (1985) *Cell* **40,** 9–17.
11. Fitzgerald, D. W., and Coleman, J. E. (1991) *Biochemistry* **30,** 5195–5201.
12. Rich, A., and RajBhandry, U. L. (1976) *Ann. Rev. Biochem.* **45,** 805–860.
13. Robillard, G. T., Carr, C. E., Vosman, F., and Reid, B. R. (1977) *Biochemistry* **16,** 5261–5273.
14. Essink, B. B. O., Das, A. T., and Berkout, B. (1995) *J. Biol. Chem.* **270,** 23867–23874.
15. Barat, C., LeGrice, S. F. J., and Darlix, J. L. (1991) *Nucleic Acids Res.* **19,** 751–757.
16. Rubin, J. R., Sabat, M., and Sundaralingham, M. (1983) *Nucleic Acids Res.* **11,** 6571–6586.
17. Tukalo, M. A., Kubler, M.-D., Kern, D., Mongel, M., Ehresman, C., Ebel, J.-P., Ehresman, B., and Giegé, R. (1987) *Biochemistry* **26,** 5200–5208.
18. Petsko, G. A. (1985) *Methods Enzymol.* **114,** 147–156.
19. Petsko, G. A., Philips, D. C., Williams, R. J. P., and Wilson, I. A. (1978) *J. Mol. Biol.* **120,** 345–359.
20. Summers, M. F., Henderson, L. E., Chance, M. R., Bess, J. W., Jr., South, T. L., Blake, P. R., Sagi, I., Perez-Alvarado, G., Sowder, R. C., II, Hare, D. R., and Arthur, L. O. (1992) *Protein Sci.* **1,** 563–574.
21. South, T. L., and Summers, M. F. (1993) *Protein Sci.* **2,** 3–19.
22. de Rocquigny, H., Gabus, C., Vincent, A., Fournié-Zaluski, M.-L., Roques, B., and Darlix, J.-L. (1992) *Proc. Natl. Acad. Sci. USA* **89,** 6472–6476.
23. Campbell, S., and Vogt, V. M. (1995) *J. Virol.* **69,** 6487–6497.